Journal of Microbiological Methods 162 (2019) 86–95

Contents lists available at ScienceDirect

Journal of Microbiological Methods

journal homepage: www.elsevier.com/locate/jmicmeth

Comparison of real-time PCR and droplet digital PCR for the detection of *Xylella fastidiosa* in plants

Enora Dupas[a,b,*], Bruno Legendre[a], Valérie Olivier[a], Françoise Poliakoff[a], Charles Manceau[a], Amandine Cunty[a]

[a] French Agency for Food, Environmental and Occupational Health & Safety, Plant Health Laboratory, Angers, France
[b] IRHS, INRA, Agrocampus-Ouest, Université d'Angers, SFR 4207 QuaSaV, 49071 Beaucouzé, France

ARTICLE INFO

Keywords:
Xylella fastidiosa
ddPCR
Molecular diagnostics
Quarantine plant pathogenic bacteria

ABSTRACT

Xylella fastidiosa (*Xf*) is a quarantine plant pathogen bacterium originating from the Americas and that has emerged in Europe in 2013. *Xf* can be detected directly on plant macerate using molecular methods such as real-time PCR, which is a sensitive technique. However, some plants may contain components that can act as PCR reaction inhibitors, which can lead to false negative results or an underestimation of the bacterial concentration present in the analyzed plant sample. Droplet digital PCR (ddPCR) is an innovative tool based on the partitioning of the PCR reagents and the DNA sample into thousands of droplets, allowing the quantification of the absolute number of target DNA molecules present in a reaction mixture, or an increase of the detection sensitivity. In this study, a real-time PCR protocol, already used for *Xf* detection in the framework of official surveys in the European Union, was transferred and optimized for *Xf* detection using ddPCR. This new assay was evaluated and compared to the initial real-time PCR on five plant matrices artificially inoculated and on naturally infected plants. In our conditions, this new ddPCR enabled the detection of *Xf* on all artificially inoculated plant macerates with a similar limit of detection, or a slight benefit for *Quercus ilex*. Moreover, ddPCR improved diagnostic sensitivity as it enabled detection of *Xf* in samples of *Polygala myrtifolia* or *Q. ilex* that were categorized as negative or close to the limit of detection using the real-time PCR. Here, we report for the first time a ddPCR assay for the detection of the bacterium *Xf*.

1. Introduction

Xylella fastidiosa (*Xf*) is a plant pathogenic bacterium known worldwide. Located in the xylem vessels of plants, its natural way of transmission is sap-feeding insect vectors (Almeida and Nunney, 2015). To date, five different subspecies (subsp.) have been described: subsp. *fastidiosa*, subsp. *morus*, subsp. *multiplex*, subsp. *pauca*, and subsp. *sandyi* (Nunney et al., 2014; Schaad et al., 2004; Schuenzel et al., 2005). In Europe, *Xf* was first detected in Italy, in the Apulia area in 2013, where the subsp. *pauca* was identified on olive trees (Saponari et al., 2013). Then, in France in 2015 (Corsica and in French Riviera region), the subsp. *multiplex* was reported firstly on *Polygala myrtifolia* and then on a large range of ornamental or wild plants (Denancé et al., 2017). More recently in 2016, the subsp. *fastidiosa*, *multiplex* and *pauca* were identified in the Balearic Islands (Spain), on olive trees, grapevines and sweet cherry trees; and in 2017, the presence of the subsp. *multiplex* was also identified in Spain near Alicante, on almond trees (Landa, 2017). Currently, 563 plant species distributed in 82 botanical families are reported to be hosts of *Xf*, and this list includes plants of major socio-economic interest such as olive trees, citrus or grapevine (EFSA, 2018). Since 2017, *Xf* has been classified in Annex I/A2 of Council Directive 2000/29/EC revised in 2017, and in the A2 list of the EPPO as a quarantine pathogen present on the EU territory and requiring mandatory control (C/2017/4883, 2017; EPPO, 2018a).

Since its detection in Italia, *Xf* has proven to be a threat to European plant production. In the Apulia Region, the infected area increased from 8000 to 715,000 ha between 2013 and 2018 (Saponari et al., 2019). This led, in 2015, to the area becoming a containment zone instead of an eradication zone. In 2018, this area covered 36% of the region and threatened about 21 million olive trees. In mainland Spain, since the first identification of *Xf*, the infected area has extended to 87,800 ha and 47 almonds orchards have been found positive for *Xf* (Bucci, 2018). Spain being the world's second largest producer of almonds with 255,503 tons produced in 2017, *Xf* could become a threat to the world almond production (FAOSTAT, 2017). In France, in Corsica, 350 foci were identified in 2017. As the infection could not be stopped, this has

* Corresponding author at: French Agency for Food, Environmental and Occupational Health & Safety, Plant Health Laboratory, Angers, France.
E-mail address: enora.dupas@anses.fr (E. Dupas).

https://doi.org/10.1016/j.mimet.2019.05.010
Received 19 March 2019; Received in revised form 20 May 2019; Accepted 20 May 2019
Available online 22 May 2019
0167-7012/

led to the declaration of the entire island as area under containment (Implementation Decision 2017/2352, 2017). Risk models predicted that in the South-East the lower part of the Durance basin and the Rhône valley were moderate to high risk areas for *Xf* infection (Martinetti and Soubeyrand, 2019). All these regions, known for their production of citrus, vines, olive trees or fruit orchards, are of great economic value for France. As no therapeutic solution has been found to control the disease, early detection and eradication of outbreaks are essential to prevent the spread of *Xf* in Europe.

As isolation and cultivation of *Xf* is fastidious, detection and identification tests are applied directly on plant extracts (Denancé et al., 2017). Nowadays, different molecular tools targeting specific DNA regions are available to detect the bacterium at the species level or to specifically detect one of the subspecies. Conventional PCRs such as Minsavage et al. (1994) have been developed, but they are less sensitive than Real-Time PCR (Baldi and La Porta, 2017). Among the real-time PCR techniques developed, the method designed by Harper et al. (2010) was identified as one of the most suitable methods for *Xf* detection. It allow to detect all the *Xf* subspecies, its limit of detection determined on different plant species is low, it is sensitive, and no cross-reactions with other bacterial species have been reported (Francis et al., 2006; Harper et al., 2010; Li et al., 2013; Modesti et al., 2017; Ouyang et al., 2013).

Even though real-time PCR is very sensitive in most cases, low bacterial contamination levels of plants and the presence of PCR inhibitors can lead to false negative results, and the underestimation of positive samples for some plant species (Modesti et al., 2017; Schrader et al., 2012). These PCR inhibitors include polyphenols, polysaccharides, pectin and xylan (Harper et al., 2010; Schrader et al., 2012; Wei et al., 2008). Studies have revealed that the improvement of DNA extraction methods, or the addition of bovine serum albumin (BSA) during the PCR assay, may reduce the impact of PCR inhibitors (Harper et al., 2010; Schrader et al., 2012). For some plants, such as *Nerium oleander*, *Prunus dulcis* and *Vitis vinifera*, a tenfold dilution prevented PCR inhibition and led to successful detection of *Xf* (Francis et al., 2006; Minsavage et al., 1994; Modesti et al., 2017). However, DNA dilution cannot be applied to every sample, due to low *Xf* concentrations in some infected plants. It can therefore be rather difficult to find a universal method, because of the wide range of *Xf* host plants. Moreover, even though real-time PCR produces quantitative data when using a calibration curve, the results are often only interpreted qualitatively for *Xf* detection (Cruaud et al., 2018; Modesti et al., 2017).

Digital PCR was set up in 1999 by Vogelstein and Kinzler and named later by Morley in 2014. By compartmentalizing the PCR reaction into thousands of droplets, ddPCR offers the promises of absolute quantification without the need for calibration (Hindson et al., 2011; Huggett et al., 2013; Morley, 2014; Voegel and Nelson, 2018; Vogelstein and Kinzler, 1999). At first, ddPCR was designed to identify rare mutations in a small number of cells (Vogelstein and Kinzler, 1999). Already used for medical purposes (Bharuthram et al., 2014; Cao et al., 2015; Hindson et al., 2011; Nixon et al., 2014; Ramírez et al., 2019), this method was transferred as a detection and quantification tool to other fields, such as environmental sciences (Doi et al., 2015; Hoshino and Inagaki, 2012), food safety control (Bian et al., 2015; Wang et al., 2018), GMO detection (Košir et al., 2017; Morisset et al., 2013) or the agronomic field (Dreo et al., 2014; Maheshwari et al., 2017; Rački et al., 2014; Voegel and Nelson, 2018; Zhao et al., 2016). The transfer of real-time PCR assays to ddPCR assays has already provided successful results for the detection and the quantification of plant pathogenic bacteria (Dreo et al., 2014; Lu et al., 2019; Maheshwari et al., 2017; Zhao et al., 2016). For example, ddPCR was more efficient than real-time PCR to detect low concentrations of *Ralstonia solanacearum* in potatoes (Dreo et al., 2014). It also increased the detection threshold of other pathogens such as *Xanthomonas citri* subsp. *citri* in citrus, Pepper mild mottle virus in plants, soil and water, or of GMOs in maize seed powder (Morisset et al., 2013; Rački et al., 2014; Zhao et al., 2016). ddPCR was reported to be up to 1000 fold more sensitive than conventional PCR developed to detect adenovirus in live attenuated vaccines (Dong et al., 2018). It allows the detection and quantification of pathogen abundance, such as *Agrobacterium vitis* in grapevines, for which previous methods lacked sensitivity (Voegel and Nelson, 2018). An additional advantage of ddPCR is its tolerance to PCR inhibitors present in plants, soil, water or food (Cao et al., 2015; Maheshwari et al., 2017; Morisset et al., 2013; Rački et al., 2014; Zhao et al., 2016). ddPCR presents many advantages that could make it an alternative for *Xf* detection.

The aim of this study was to transfer the real-time PCR developed by Harper et al. (2010) into a ddPCR assay, in order to improve the detection of *Xf* at low concentrations in plant matrices rich in PCR inhibitors. ddPCR was compared to real-time PCR using five artificially inoculated plant matrices and naturally infected plants sampled in France. The plant species used as matrices were selected for their level of PCR inhibitors reported by the Plant Health Laboratory (PHL) of the French Agency for Food, Environmental and Occupational Health & Safety (ANSES) following the analysis of thousands of different plant samples collected since 2015 in the context of the national *Xf* survey in France (personal communication, Bruno Legendre). *Polygala myrtifolia* was selected as a matrix containing a low concentration of inhibitors, *Lavandula angustifolia*, *Olea europaea, Quercus ilex* and *Rosmarinus officinalis* were selected as matrices containing high concentrations of inhibitors. Experimental assays were set up following the standard PM7/98 and the digital MIQE guidelines. The following performance criteria were evaluated: analytical sensitivity, repeatability, and diagnostic specificity (EPPO, 2014; Huggett et al., 2013).

2. Materials and methods

2.1. Bacterial strains

Bacterial strains *Xf* subsp. *multiplex* CFBP 8416, isolated in France (Corsica) in 2015 from symptomatic *P. myrtifolia* (Denancé et al., 2017) and *Xf* subsp. *fastidiosa* CFBP 7970, isolated in the United States (Florida) from *Vitis vinifera* were cultivated on modified PWG media at 28 °C for two weeks (EPPO, 2018b). Bacterial suspensions of pure culture of *Xf* were prepared in sterile demineralized water and suspensions titer was estimated by immunofluorescence (IF) (EPPO, 2018b, 2009). The antiserum, used to count *Xf,* was especially produced in collaboration with the UR1268 BIA - Team Allergy of the French National Institute for Agricultural Research (INRA) of Angers-Nantes. It resulted from the inoculation of rabbits with nine strains of *Xf* chosen to be as diverse as possible in terms of subspecies, geographical location, and host plant species. The initial concentration of the CFBP 8416 bacterial suspension was estimated by IF at 1.84×10^9 bacteria/mL (b/mL). This suspension was used to spike all the artificially inoculated samples in this study. The bacterial suspension of the strain CFBP 7970 was calibrated at 1×10^7 b/mL and used as a positive control for the PCR reactions.

2.2. Plant materials

Healthy plant materials used for spiking assays were collected in 2018. *L. angustifolia*, *O. europaea*, *Q. ilex*, *R. officinalis* were sourced from Maine-et-Loire, a French department known to be *Xf* free. *P. myrtifolia* was produced in a nursery in Brittany (*Xf* free) and had a European phytosanitary passport certifying its healthy status. Moreover, no symptoms were recorded on these five plants. In this study, the healthy status of the five matrices was first checked using the real-time PCR assay Harper et al. (2010).

Naturally infected samples of *Calicotome* sp. (one sample), *L. angustifolia* (four samples), *P. myrtifolia* (13 samples), and *Q. ilex* (4 samples) were collected in the context of the national survey, between 2016 and 2018 in Corsica and in the PACA region of France. These 22 samples were already found to have a positive status or to be at the limit of detection by the PHL, using the real-time PCR developed by Harper et al. (2010).

2.3. Plant spiking

The artificially inoculated plant samples were prepared by mixing 1 g of healthy plant petiole in 4.5 mL of sterile demineralized water and spiked with 0.5 mL of a known concentration of bacterial suspension. Each matrix was spiked in order to reach a range dilution of 1×10^5 b/mL; 5×10^4 b/mL; 1×10^4 b/mL; 5×10^3 b/mL; 1×10^3 b/mL; 5×10^2 b/mL; and 1×10^2 b/mL. The negative template control (NTC) was obtained by mixing 1 g of healthy plant petiole with 5 mL of sterile demineralized water.

2.4. DNA extraction

The bacterial strain suspension used as a positive control for all the PCRs was inactivated by thermal lysis. A volume of 1 mL of bacterial suspension was heated at 100 °C for 5 min and then frozen at −20 °C for at least 15 min.

The plants to be spiked and the naturally infected samples were homogeneously crushed in an extraction bag (Bioreba AG, Basel, Switzerland) with a pneumatic press prior DNA extraction. Extraction, washing, and elution of the DNA were automated using KingFisher™ mL (Thermo Scientific). DNA extracts were kept at 4 °C for a week, or stored at −20 °C for a longer period.

2.5. Real-time PCR Harper et al., 2010

The real-time PCR assays were performed on the thermal cycler CFX96 real-time System C1000 Touch (Bio-Rad), using 96-well plates (Hard-Shell® 96-Well PCR Plates, #hsp9601, Bio-Rad). The following thermal cycling program used was: 50 °C for 2 min, 94 °C for 10 min, then 40 cycles of two step of 94 °C for 10 s and 62 °C for 40 s. The reaction mix was prepared in a final volume of 20 µL containing: 1× TaqMan Fast Universal Master Mix (Applied Biosystems), 300 nM of each *Xf* forward and reverse primers (*XF*-F and *XF*-R, respectively), 100 nM of 6'FAM/BHQ-1 labeled probe (*XF*-P), 300 µg/µL of BSA, and 2 µL of DNA sample. 2 µL of lysed suspension of the strain CFBP 7970 at 1×10^7 b/mL was added as positive control for each PCR run. Two negative controls were used: a) sterile demineralized water, b) the extracted DNA from each healthy plant previously artificially inoculated with sterile demineralized water. For the artificially contaminated plant material, each sample was amplified in triplicate and on three independent PCR runs to obtain nine Ct values per sample. For the naturally infected plant material, each sample was amplified in duplicate on the same PCR run.

The data acquisitions and data analyses were performed using Bio-Rad CFX Manager, v 3.0. The determination of Ct values is done using the regression mode of the software, which applies a multivariable, nonlinear regression model to individual well traces and then uses this model to compute an optimal Ct value (Bio-Rad, 2008). This allowed all Ct results to be compared within and between PCR plates. A Ct higher than 38 was considered to be a negative result, according to the cut-off indicated by (Harper et al., 2010). For all the following analyses, the limit of detection was fixed at 100%, meaning the lowest concentration at which all replicates gave a positive signal. The efficiency of the real-time PCR amplification was estimated from the slope of each standard curve using the equation: $E = -1 + 10^{(-1/\text{slope})}$.

2.6. Optimization and evaluation of the ddPCR assay

Two thermal gradients were tested to determine the optimal hybridization temperature ranging from 54.6 to 64.6 °C, and from 57 to 62 °C. Thermal gradients were applied on samples of *P. myrtifolia*, spiked with suspensions of *Xf* ranging from 1×10^5 b/mL to 1×10^3 b/mL. BSA was tested at the concentration determined by Harper et al. (2010) (300 µg/µL) on a sample of *P. myrtifolia* spiked with *Xf* at a concentration of 1×10^5 b/mL. In order to optimize the assay for the five matrices spiked at 1×10^5 b/mL, four different DNA volumes added to the reaction mix were tested: 2 µL; 4 µL; 6 µL and 8 µL. Using the optimized protocol, tenth dilutions of L. *angustifolia* and *R. officinalis* spiked with 1×10^3 b/mL were tested. All the experiments conducted to optimize the ddPCR assay were amplified in triplicate. For each ddPCR assay the positive and negative controls used were the same as for the qPCR described above.

2.7. Optimized ddPCR assay

The optimized ddPCR reaction mix conditions retained were a final reaction volume of 20 µL containing: 1× ddPCR™ Supermix for Probes (No dUTP) (Bio-Rad), 900 nM *Xf* forward and reverse primers (*XF*-F and *XF*-R), 250 nM 6'FAM/BHQ-1 labeled probe (*XF*-P), and 8 µL of DNA sample. Droplets were generated with the QX200™ Droplet Digital™ System (Bio-Rad) in a cartridge containing 20 µL of the reaction mix and 70 µL of Droplet Generation Oil for Probes (ddPCR™ 96-Well Plates #12001925, Bio-Rad). The entire emulsion volume was transferred from the cartridge to a 96-well PCR plate (Bio-Rad) and the PCRs were performed on the thermal cycler CFX96 real-time System C1000 Touch (Bio-Rad). Optimal thermocycling conditions retained were: DNA polymerase activation of 95 °C for 10 min, then 40 cycles of two-steps of 94 °C for 30 s for denaturation and 59 °C for 60 s for hybridization and elongation, followed by a final step at 98 °C for 10 min for droplet stabilization. According to Bio-Rad recommendations, a temperature ramp of 2 °C/s was fixed on all PCR steps and the lead was heated at 105 °C. After amplification, the PCR plate was directly transferred to the droplet reader QX200™ Droplet Digital™ System (Bio-Rad). QuantaSoft 1.7.4.0917 software was used for data acquisition and data analysis. The entire concentration range of spiked matrices was first amplified in triplicate on the same run. Then, for each matrix, samples with concentrations equal to and below the limit of detection identified by real-time PCR were amplified in triplicate on two other independent runs, in order to ultimately obtain nine results for these samples. Finally, the amplifications of the naturally infected samples were performed in one replicate in one run.

2.8. ddPCR analysis

Data were analyzed directly with QuantaSoft™ Analysis Pro software. For each plate and each matrix, a threshold was manually set up just above the amplitude value of the cloud corresponding to the negative droplets, also considered as the background, and according to the results of the corresponding NTC (Lievens et al., 2016). This threshold enabled the differentiation of droplets by categorizing them as positive (high level of fluorescence) or negative (low and constant level of fluorescence). The PCR reactions with fewer than 10,000 droplets generated were excluded from the analysis, and a result was considered positive if at least two positive droplets were detected. The software provided the results in target copies by reaction using the following formula:

$$C = -\ln\left(1 - \frac{P}{P+N}\right) * \frac{1}{V}$$

where C corresponded to the concentration in target DNA copies/well (cp/well), P the positive droplet number, N the negative droplet number, and V the mean volume in µL of one droplet. According to Bio-Rad, V is equal to 0.85×10^{-3} µL. Primers and probe targeted a part of the *rimM* gene, which is present in a single copy in the *Xf* genome. Therefore, the result can be directly converted into cp/µL in the initial samples, by multiplying it with the total volume of reaction mix (20 µL), and then dividing it by the volume of DNA sample added to the reaction mix (8 µL) at the beginning of the assay.

A bias, meaning the under or over-estimation of the quantification estimated by ddPCR, in comparison with the expected concentration, was calculated with the following formula:

$$Bias = \frac{detected\ DNA\ amount - assumed\ DNA\ provided}{assumed\ DNA\ provided} * 100$$

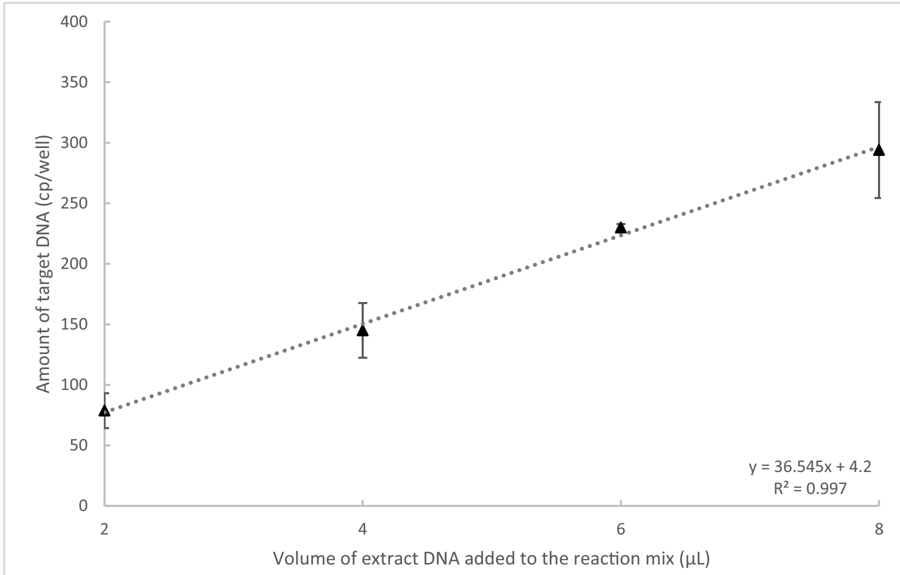

Fig. 1. Influence of the DNA extract volume added to the ddPCR reaction mix on the amount of DNA target detected for *O. europaea*.

Table 1
Mean Ct values obtained with real-time PCR for the bacterial suspension and the five spiked plant matrices.

Dilution range (b/mL)	Bacterial suspension		*L. angustifolia*		*O. europaea*		*P. myrtifolia*		*Q. ilex*		*R. officinalis*	
1×10^5	32.18 ± 0.38[a]	(9)[b]	30.76 ± 0.18	(9)	36.02 ± 0.43	(9)	30.38 ± 0.17	(9)	31.85 ± 0.10	(9)	32.24 ± 0.17	(9)
5×10^4	33.14 ± 0.45	(9)	31.24 ± 0.11	(9)	36.59 ± 0.99	(9)	31.41 ± 0.18	(9)	32.00 ± 0.15	(9)	32.53 ± 0.14	(9)
1×10^4	35.46 ± 0.64	(9)	33.68 ± 0.20	(9)	37.32 ± 0.05	(3)	33.85 ± 0.34	(9)	34.90 ± 0.50	(9)	34.83 ± 0.66	(9)
5×10^3	35.55 ± 0.21	(9)	34.93 ± 0.20	(9)	37.86 ± 0.49	(2)	34.59 ± 0.28	(9)	35.31 ± 0.55	(9)	36.09 ± 1.05	(9)
1×10^3	37.42 ± 0.37	(6)	37.45 ± 0.58	(9)	37.78 ± 0.53	(2)	38.00 ± 0.56	(9)	37.62 ± 0.86	(7)	38.05 ± 0.50	(6)
5×10^2	38.81 ± 0.12	(5)	37.44 ± 0.00	(1)	36.61 ± 0.00	(1)	37.62 ± 0.18	(5)	37.76 ± 0.29	(4)	38.25 ± 0.13	(4)
1×10^2	38.00 ± 0.19	(6)	38.46 ± 1.01	(2)	nd	(0)	38.29 ± 0.13	(4)	36.75 ± 0.19	(6)	nd	(0)
0	nd[c]	(0)	nd	(0)	nd	(0)	nd	(0)	nd	(0)	nd	(0)

[a] Average Ct ± Standard Deviation (SD).
[b] Number of positive replicates on nine replicates analyzed.
[c] Not detected.

Table 2
Curve information for the *Xf* bacterial suspension and the five *Xf* spiked plant matrices.

	Curve equation	R^2
ddPCR		
Bacterial suspension	y = 0.41× + 1136.66	0.99
L. angustifolia	y = 0.85× + 2007.35	0.96
O. europaea	y = 0.02× + 1016.11	1.00
P. myrtifolia	y = 0.90× − 781.02	1.00
Q. ilex	y = 0.36× + 1187.91	0.99
R. officinalis	y = 0.37× + 1363.74	0.98

	Curve equation	R^2	Efficiency
Real-time PCR			
Bacterial suspension	y = −2.75× + 46.06	0.97	131.01%
L. angustifolia	y = −3.43× + 47.61	0.99	95.68%
O. europaea	y = −1.89× + 45.49	0.98	238.14%
P. myrtifolia	y = −3.71× + 48.80	0.99	86.01%
Q. ilex	y = −3.02× + 46.66	0.98	114.35%
R. officinalis	y = −3.05× + 47.18	0.99	112.75%

3. Results

3.1. Optimization of the ddPCR assay

The ddPCR appeared to be efficient for *Xf* detection at all tested temperatures. The first thermal gradient tested allowed us to identify 58.5 °C as the most suitable hybridization temperature, for which positive droplets showed the highest fluorescence amplitude and were well distinguished from the negative droplets. The second thermal gradient confirmed this preliminary result and made it possible to fix the optimum hybridization temperature for ddPCR at 59 °C. At this temperature, positive droplets presented the highest fluorescence

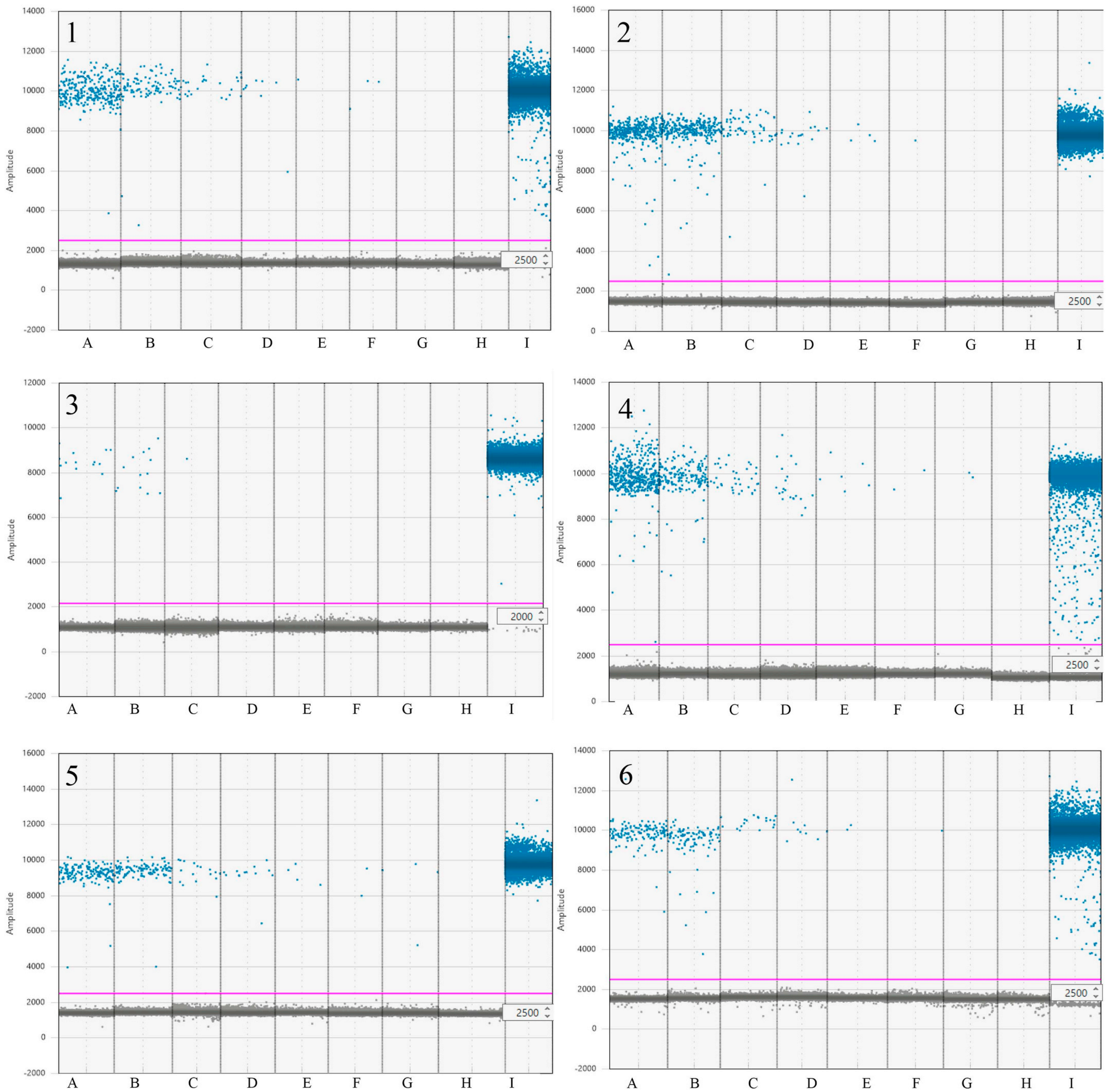

Fig. 2. Comparison of the different limits of detection of *Xf* obtained by ddPCR in the bacterial suspension and spiked plant matrices. Pink line: threshold separating negative from positive droplets. Blue dots: positive droplets with amplification. Grey dots: negative droplets with no amplification. 1: Bacterial suspension. 2: *Lavandula* sp. 3: *O. europaea*. 4: *P. myrtifolia*. 5: *Q. ilex*. 6: *R. officinalis*. Wells A to G bacterial suspension range of *Xf*, A: 1×10^5 b/mL; B: 5×10^4 b/mL; C: 1×10^4 b/mL; D: 5×10^3 b/mL; E: 1×10^3 b/mL; F: 5×10^2 b/mL and G: 1×10^2 b/mL. Well H: NTC specific to each matrix. Well I: positive control (lysis suspension of 1×10^7 b/mL of *Xf*).

amplitude, the less "rain" (i.e. droplets ranging between the positive and negative ones), and better separation from negative droplets (data not shown).

Addition of BSA to the reaction mix did not increase the number of droplets amplified, the number of target DNA detected, nor the amplitude of the fluorescence signal. However, as it increased the standard deviation between replicates, no BSA was added for the optimized ddPCR protocol retained in this study (data not shown).

Like for *O. europaea* shown in Fig. 1, *Xf* detection was successful for all the five matrices, regardless of the volume of DNA extract added to the PCR mix (Supplemental Data 1). The increase of the DNA volume in the mix has improved the sensitivity of the DNA copy detection. Nevertheless, the presence of inhibitors could be highlighted in *Q. ilex* and *R. officinalis* as the amount of target DNA detected was not proportional with the volume of DNA tested. As the aim of the ddPCR assay in this study was also to improve the limit of detection of *Xf* in low-level contaminated samples, the final volume of DNA chosen was 8 µL. This corresponded to the highest volume of DNA that could be added to ddPCR reaction mix in this study.

A tenth dilution of the DNA of L. *angustifolia* and *R. officinalis* spiked

Table 3
Mean concentrations estimated in copies/mL (cp/mL) obtained with ddPCR for the bacterial suspension and the five spiked plant matrices.

Dilution range (b/mL)	Bacterial suspension		*L. angustifolia*		*O. europaea*		*P. myrtifolia*		*Q. ilex*		*R. officinalis*	
1×10^5	4.02×10^4 [a] $\pm 3.63 \times 10^3$	(3/3)[b]	$8.07 \times 10^4 \pm 3.70 \times 10^3$	(3/3)	$3.38 \times 10^3 \pm 5.67 \times 10^2$	(9/9)	$9.08 \times 10^4 \pm 4.95 \times 10^3$	(3/3)	$3.58 \times 10^4 \pm 2.96 \times 10^3$	(3/3)	$3.62 \times 10^4 \pm 3.71 \times 10^3$	(3/3)
5×10^4	$2.53 \times 10^4 \pm 2.20 \times 10^3$	(3/3)	$5.81 \times 10^4 \pm 2.02 \times 10^3$	(3/3)	$2.20 \times 10^3 \pm 5.45 \times 10^2$	(9/9)	$4.03 \times 10^4 \pm 4.71 \times 10^3$	(3/3)	$2.30 \times 10^4 \pm 9.92 \times 10^2$	(3/3)	$2.38 \times 10^4 \pm 3.20 \times 10^3$	(3/3)
1×10^4	$5.73 \times 10^3 \pm 1.14 \times 10^3$	(3/3)	$1.17 \times 10^4 \pm 2.19 \times 10^3$	(3/3)	$5.28 \times 10^2 \pm 1.90 \times 10^2$	(4/9)	$6.17 \times 10^3 \pm 1.39 \times 10^3$	(3/3)	$4.95 \times 10^3 \pm 4.04 \times 10^2$	(3/3)	$5.49 \times 10^3 \pm 2.98 \times 10^2$	(3/3)
5×10^3	$2.84 \times 10^3 \pm 8.78 \times 10^2$	(9/9)	$4.85 \times 10^3 \pm 1.21 \times 10^3$	(3/3)	$4.25 \times 10^2 \pm 0.00$	(1/9)	$5.14 \times 10^3 \pm 1.48 \times 10^3$	(3/3)	$2.81 \times 10^3 \pm 7.90 \times 10^2$	(9/9)	$3.78 \times 10^3 \pm 2.16 \times 10^3$	(9/9)
1×10^3	$8.54 \times 10^2 \pm 2.57 \times 10^2$	(9/9)	$5.66 \times 10^2 \pm 1.63 \times 10^2$	(6/9)	No Call	(0/9)	$6.80 \times 10^2 \pm 2.68 \times 10^2$	(9/9)	$1.07 \times 10^3 \pm 5.58 \times 10^2$	(9/9)	$9.04 \times 10^2 \pm 1.61 \times 10^2$	(7/9)
5×10^2	$6.20 \times 10^2 \pm 1.19 \times 10^2$	(8/9)	No Call	(0/9)	No Call	(0/9)	$5.15 \times 10^2 \pm 1.43 \times 10^2$	(4/9)	$7.17 \times 10^2 \pm 2.59 \times 10^2$	(7/9)	$6.18 \times 10^2 \pm 4.56 \times 10^2$	(5/9)
1×10^2	$5.84 \times 10^2 \pm 2.06 \times 10^2$	(6/9)	$3.73 \times 10^2 \pm 0.00$	(1/9)	No Call	(0/9)	$1.77 \times 10^2 \pm 0.00$	(1/9)	$6.23 \times 10^2 \pm 1.50 \times 10^2$	(7/9)	$2.01 \times 10^2 \pm 2.92 \times 10^1$	(2/9)
0	No Call	(0/9)	No Call	(0/9)	No Call	(0/9)	No Call	(0/9)	No Call	(0/9)	No Call	(0/9)

[a] Average Ct ± SD.
[b] Number of positive replicates/number of replicates analyzed.

Table 4
Comparison of real-time PCR (mean Ct values) and ddPCR (cp/mL) for the detection of Xf in naturally infected samples.

Matrices	Sample name	real-time PCR Ct means	ddPCR concentration (cp/mL)
Calicotome sp	C01	36.41 (1/2)[a]	NA (1/12618)[b]
L. angustifolia	L01	26.08 (2/2)	1.59E+06 (6614/15814)
L. angustifolia	L02	26.69 (2/2)	8.82E+05 (3581/13826)
L. angustifolia	L03	31.39 (2/2)	3.65E+04 (196/15,876)
L. angustifolia	L04	31.78 (2/2)	4.19E+04 (227/16056)
P. myrtifolia	P01	23.30 (2/2)	1.61E+07 (17,615/17,690)
P. myrtifolia	P02	25.04 (2/2)	4.12E+06 (11,714/15,550)
P. myrtifolia	P03	26.90 (2/2)	1.28E+06 (5896/16720)
P. myrtifolia	P04	27.25 (2/2)	9.52E+05 (4395/15894)
P. myrtifolia	P05	28.10 (2/2)	5.24E+05 (2895/17733)
P. myrtifolia	P06	28.44 (2/2)	5.70E+05 (2985/16936)
P. myrtifolia	P07	28.80 (2/2)	2.39E+05 (1446/18565)
P. myrtifolia	P08	29.48 (2/2)	2.11E+05 (1272/18376)
P. myrtifolia	P09	31.20 (2/2)	5.38E+04 (296/16332)
P. myrtifolia	P10	32.21 (2/2)	3.66E+04 (216/17459)
P. myrtifolia	P11	35.64 (2/2)	2.63E+03 (16/17898)
P. myrtifolia	P12	37.00 (2/2)	8,56E+02 (3/10309)
P. myrtifolia	P13	38.65 (2/2)	3,25E+03 (12/10848)
Q. ilex	Q01	32.29 (2/2)	2.13E+04 (113/15673)
Q. ilex	Q02	34,85 (2/2)	1,02E+04 (39/11269)
Q. ilex	Q03	35,80 (2/2)	3,21E+03 (13/11925)
Q. ilex	Q04	39.00 (1/2)	4,41E+02 (2/13340)

[a] Number of replicates positive for *Xf* detection/total number of analyzed replicates.
[b] Number of positive droplets/total number of droplets (i.e. positives and negatives).

with 1×10^3 b/mL, corresponding to the first concentration under the limit of detection obtained with ddPCR, was tested. For L. *angustifolia*, none of the six replicates provided positive droplets. In only one of the six replicates tested for *R. officinalis,* two positive droplets were detected. Dilution of the DNA extract of L. *angustifolia* and *R. officinalis* did not improve the limit of detection or was not reproducible enough in this study.

3.2. *Xf* detection by ddPCR in spiked plant samples

The healthy status of the five plants was validated before spiking, by applying real-time PCR Harper et al. (2010). Indeed, no Ct value was obtained for all the five plant matrices (Table 1). As expected, in these assays, no cross-reaction was found, as no positive droplets were found for any of the NTCs, for the plant matrices. Regression curves were constructed to reveal the relationship between the expected concentration versus the measured concentration. All the ddPCR matrix standard curves showed high linearity as the correlation coefficient (R^2) was higher than 0.96 (supplemental data 2). This indicated the successful outcomes and good performances of all the assays (Table 2).

The results obtained for the five matrices and the bacterial suspension showed clear distinctions between positive (blue) and negative (grey) droplets (Fig. 2). The background (negative droplets) had a similar fluorescence amplitude between samples of the same matrix, and between the five matrices (mean amplitude of fluorescence of negatives droplets ranged from 1070 to 1606). The threshold was manually set at an amplitude of fluorescence between 2000 and 3000 for each ddPCR run. Compared to the positive control, which is a lysed suspension of pure culture of *Xf*, very less rain was observed on the spiked sampled plots, showing high efficiency of the PCR reactions.

ddPCR enabled the detection of *Xf* in all the matrices, but at different concentrations (Table 3). The limit of detection was fixed at 5×10^4 b/mL, i.e., 2.5×10^5 b/g of plant for *O. europaea*, at 5×10^3 b/mL, i.e., 2.5×10^4 b/g of plant for L. *angustifolia* and *R. officinalis,* and at 1×10^3 b/mL, i.e., 5×10^3 b/g of plant for *Q. ilex*, *P. myrtifolia* and

Table 5
Concordance between ddPCR and real-time PCR results on the 22 naturally infected samples.

		Samples analyzed with ddPCR		
		Positive results	Negative results	
Samples analyzed with real-time PCR	Positive results	19	1	20
	Negative results	2	0	2
		21	1	22

the bacterial suspension. The bias between the detected amount of DNA and the presumed amount of DNA provided was calculated for each matrix at the limit of detection. Compared to the quantity of DNA expected, DNA quantifications of *Xf* were overestimated by 6.54% and 23.96% in *Q. ilex* and in the bacterial suspension, respectively. In L. *angustifolia*, *R. officinalis*, *P. myrtifolia*, and *O. europaea*, the DNA quantifications of *Xf* were underestimated by 3.08%, 24.36%, 32.03% and 95.60%, respectively.

3.3. Real-time PCR vs ddPCR for Xf detection in spiked samples

As for ddPCR, all the real-time PCR matrix standard curves showed high linearity, as the correlation coefficient (R^2) was greater than 0.97 (Table 2). This indicated the successful outcomes and good performances of all the assays. Nevertheless, with the exception of L. *angustifolia*, the efficacy range was outside the 90–100% range, indicating the presence of PCR inhibitors in these plants or incomplete extraction of target DNA.

Real-time PCR Harper et al. (2010) was used as a reference method in this study. For all the assays, no mean Ct values exceeding 38 were recorded at a concentration equal to or higher than the limit of detection, meaning that the limit of detection and positive results were consistent. Moreover, for *O. europaea* the EPPO PM 7/24 protocol mentions a limit of detection for samples artificially contaminated with *Xf* subsp. *multiplex* of 100% at 1×10^5 b/mL. In this study, the limit of detection of 5×10^4 b/mL was close to that presented in the PM 7/24 (EPPO, 2018b). The limit of detection of *Xf* in *P. myrtifolia* is known to be 1×10^3, which is the same as the value we found (Legendre B., personal communication). The limits of detection of *Xf* subsp. *multiplex* for the other matrices could not be compared, as there are no available data.

Real-time PCR and ddPCR technology provided equivalent limits of detection for *Xf* in the following matrices: *O. europaea, P. myrtifolia* and *R. officinalis* (Table 1, Table 3). The ddPCR technology presented a slightly higher limit of detection of 0.5 log for L. *angustifolia*. However, a decrease in the limit of detection for *Xf* of 0.5 log for *Q. ilex* and the bacterial suspension were observed. In the conditions of DNA extraction used for this study, and according to the volume of DNA added to the real-time PCR assay, the theoretical limit of detection should be 1×10^2 b/mL for the five plant matrices. These results revealed that L. *angustifolia* and *P. myrtifolia* may contain fewer real-time PCR inhibitors than *Q. ilex* and *R. officinalis*. Moreover, the limit of detection of the bacterial suspension was 5×10^3 b/mL, meaning that the QuickPick extraction kit may not be 100% efficient to extract the DNA of bacteria in pure culture.

3.4. Xf detection in naturally infected samples: real-time PCR vs ddPCR

A total of 22 samples from infected areas were tested using real-time PCR and ddPCR. Of these, 20 had a mean Ct value below 38 (ranging from 23.30 to 37.00) (Table 4). However, two samples, P13 and Q04, had a Ct value above 38 (38.65 and 39, respectively), and were considered negative (Table 5).

The 22 naturally infected samples were then analyzed by ddPCR. The presence of *Xf* was detected in 21 of them, including samples P13 and Q04, with at least two droplets, and a total concentration ranging from 4.41×10^2 cp/mL to 1.61×10^7 cp/mL, confirming the ability of ddPCR to detect *Xf* in naturally infected samples. As only one positive droplet was detected for sample C01, this sample was considered negative by ddPCR. With the exception of samples L04, P06 and P13, the decrease in the Ct value was correlated with an increase in the quantity of DNA detected by ddPCR (Table 4). For each matrix the results obtained by ddPCR and real-time PCR were compared and were highly correlated (Fig. 3).

4. Discussion

Since 2013, *Xf* is known to be an emergent plant pathogen in Europe (Saponari et al., 2013). In the countries where *Xf* is present, infected area are growing up every year and threaten productions of economic value (Bucci, 2018; Implementation Decision 2017/2352, 2017; Martinetti and Soubeyrand, 2019; Saponari et al., 2019). As with most plant pathogenic bacteria, no therapeutic solution has been found to kill this pathogen, in addition to vector insect control, early detection and eradication of outbreaks are the only way to prevent the spread of *Xf*. Here we present the first transfer in ddPCR of a real-time PCR protocol already used for *Xf* detection in the framework of official survey in the EU and all the setting up steps performed.

To implement appropriate control measures, a major issue is getting reliable and sensitive tools capable of early detection of *Xf*. The additional challenge of an *Xf* detection tool is its ability to detect the bacterium on its wide range of host plants, some of which are rich in PCR inhibitors. During DNA extraction, the purification step(s) can solve this problem, but inhibitors can still sometimes be co-extracted with bacterial DNA in some plant species. According to Francis et al., 2006; Minsavage et al., 1994; Modesti et al., 2017, dilutions of extracted plant DNA of plants rich in inhibitors could reduce inhibitor effect on PCR efficiency In this study, diluting the DNA extract of L. *angustifolia* and *R. officinalis* did not improve the limit of detection using ddPCR, or the obtained results were not sufficiently reproducible. This approach using ddPCR does not seem to be useful and appropriate for *Xf* detection in these two matrices. Nevertheless, more tests should be carried out to support this assumption.

Compared to real-time PCR, ddPCR can be considered as a controversial method. Some studies have revealed that ddPCR was useful to improve pathogen detection sensitivity and to decrease the impact of PCR inhibitors on PCR efficiency (Arvia et al., 2017; Bharuthram et al., 2014; Dong et al., 2018; Rački et al., 2014; Zhao et al., 2016). In other cases, ddPCR was 10 and 100 fold less sensitive than real-time PCR in detecting cytomegalovirus and *Leishmaniasis* parasite DNA, respectively (Hayden et al., 2013; Ramírez et al., 2019). Dreo et al., reported that ddPCR benefits were dependent of the pathosystem studied (Dreo et al., 2014). The detection of *Erwinia amylovora* showed similar levels using real-time PCR and ddPCR, while the detection of *R. solanacearum* in low-level infected samples was improved by ddPCR (Dreo et al., 2014). In this study, we easily transfer a real-time PCR in ddPCR with only setting up steps. Both methods showed the same limit of detection for *O. europaea, P. myrtifolia* and *R. officinalis*. Real-time PCR allowed better detection of 0.5 log for L. *angustifolia*, and ddPCR allowed better detection of 0.5 log for *Q. ilex* and bacterial suspension.

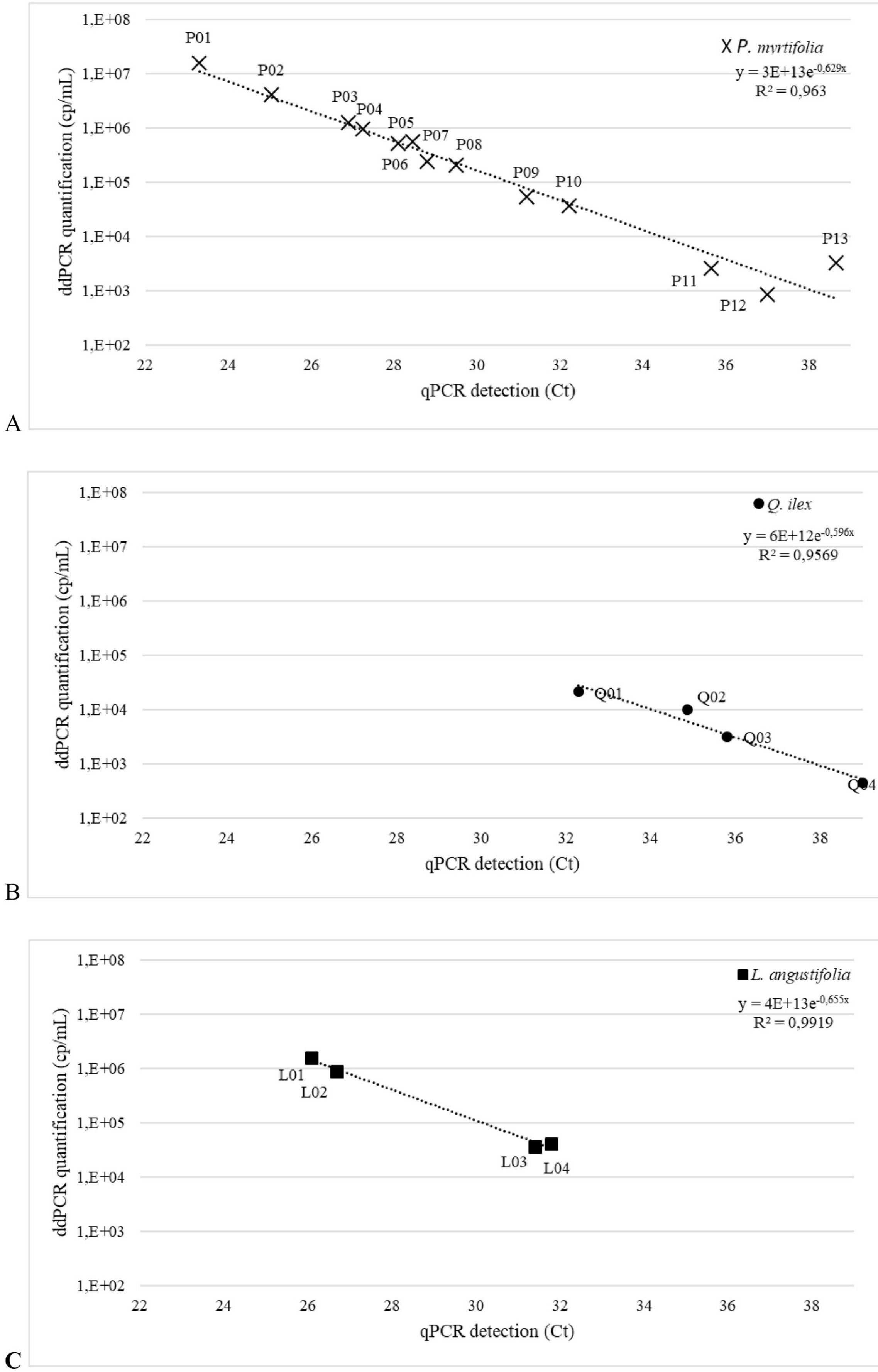

Fig. 3. Correlation between the Ct values obtained by real-time PCR and the amount of target DNA quantified by ddPCR (log cp/mL) for the naturally infected samples analyzed. A: samples of *P. myrtifolia*; B: samples of *Q. ilex*; C: samples of L. *angustifolia*.

ddPCR was also compared with real-time PCR on 22 naturally infected samples. Inhibitors seems to act similarly on real-time PCR and ddPCR. As Ct values were obtained for all samples using real-time PCR, in our study. At the exception of one sample, ddPCR confirmed the real-time PCR results. Moreover, ddPCR was more sensitive because of its low detection threshold fixed at two positive droplets. It allowed the detection of *Xf* in two samples for which their high Ct values in real-time PCR would have categorized them as negative, due to too late detection, in the framework of official survey. As shown by Dreo et al. (2014) for the detection of *R. solanacearum*, ddPCR technology could offer a real advantage for the detection of plant pathogenic bacteria, and can be applied to the detection of *Xf* in contaminated plants with low concentrations of target DNA (Dreo et al., 2014). ddPCR could contribute to better management of the epidemic and early detection of outbreaks not detected as positive by PCR in real time.

The ddPCR technology requires more steps and is more time-consuming and expensive than real-time PCR. It does not seem to be suitable for routine analysis. Furthermore, the reaction mix has to handle with care to ensure the generation of the appropriate number of droplets. Nevertheless, ddPCR is a useful technology that should be used in specific cases. ddPCR should be a new tool to confirm the status of samples that have given results at the detection limit or were classified as negative due to late Ct and come from an area where the presence of *Xf* is suspected or plants known to be rich in PCR inhibitors. As for other studies, the transfer of real-time PCR in ddPCR was easily performed (Arvia et al., 2017; Dong et al., 2018; Dreo et al., 2014), other real-time PCR used in the framework of *Xf* survey could be transferred in ddPCR, as the Francis et al., 2006 or Ouyang et al., 2013. Their use could be a confirmation tool in the case of litigation, complementary to Harper's results and targeting different parts of the genome. Conclusion

In this work, we proposed the first suitable ddPCR assay for the detection of *Xf* in plants. We easily transferred a well-known routinely used real-time PCR technique for *Xf* detection in ddPCR. Here, we reported all the set up steps leading to the optimal protocol and its comparison with the current routine method. The results demonstrated the usefulness of ddPCR technology as an alternative method for *Xf* detection in plants, as we were able to detect the bacteria until 1×10^3 b/mL in spiked samples and in naturally infected samples tested negative in real-time PCR. As only two droplets are needed to confirm a sample as positive with ddPCR, this method could confirm the status of samples found to be negative by real-time PCR due to high Ct values, and could improve *Xf* detection in low-level infected samples. In addition, as part of *Xylella* monitoring plan, the ddPCR should classify samples previously detected as undetermined (Ct value = 35 to 38) as positive and improve early detection of bacteria. However, due to its cost and the time required to conduct a assay, this technology should be reserved for the confirmation of results. ddPCR should be tested on insects to see whether this technology would still be efficient, and whether it offers a benefit for *Xf* detection in this matrix.

Acknowledgements

We thank Marie-Agnès Jacques, Philippe Reignault, Pascal Gentit and Mathieu Rolland for fruitful discussions and critical reading of the manuscript.

Funding

This work was supported by ANSES and the Inra-SPE department. Enora Dupas was co-funded by ANSES and the Inra-SPE Department.

Declarations of interest

The authors have no competing interests to declare.

Appendix A. Supplementary data

Supplementary data to this article can be found online at https://doi.org/10.1016/j.mimet.2019.05.010.

References

Almeida, R.P.P., Nunney, L., 2015. How do Plant diseases caused by Xylella fastidiosa emerge? Plant Dis. 99, 1457–1467. https://doi.org/10.1094/PDIS-02-15-0159-FE.

Arvia, R., Sollai, M., Pierucci, F., Urso, C., Massi, D., Zakrzewska, K., 2017. Droplet digital PCR (ddPCR) vs quantitative real-time PCR (qPCR) approach for detection and quantification of Merkel cell polyomavirus (MCPyV) DNA in formalin fixed paraffin embedded (FFPE) cutaneous biopsies. J. Virol. Methods 246, 15–20. https://doi.org/10.1016/j.jviromet.2017.04.003.

Baldi, P., La Porta, N., 2017. Xylella fastidiosa: host range and advance in molecular identification techniques. Front. Plant Sci. 8. https://doi.org/10.3389/fpls.2017.00944.

Bharuthram, A., Paximadis, M., Picton, A.C.P., Tiemessen, C.T., 2014. Comparison of a quantitative Real-Time PCR assay and droplet digital PCR for copy number analysis of the CCL4L genes. Infect. Genet. Evol. 25, 28–35. https://doi.org/10.1016/j.meegid.2014.03.028.

Bian, X., Jing, F., Li, G., Fan, X., Jia, C., Zhou, H., Jin, Q., Zhao, J., 2015. A microfluidic droplet digital PCR for simultaneous detection of pathogenic Escherichia coli O157 and listeria monocytogenes. Biosens. Bioelectron. 74, 770–777. https://doi.org/10.1016/j.bios.2015.07.016.

Bio-Rad, 2017. CFX96™ and CFX384™ Real-Time PCR Detection Systems Instruction Manual. vol. 184.

Bucci, E.M., 2018. Xylella fastidiosa, a new plant pathogen that threatens global farming: ecology, molecular biology, search for remedies. Biochem. Biophys. Res. Commun. 502, 173–182. https://doi.org/10.1016/j.bbrc.2018.05.073.

C/2017/4883, 2017. Commission Implementing Directive (EU) 2017/1279 of 14 July 2017 Amending Annexes I to V to Council Directive 2000/29/EC on Protective Measures against the Introduction into the Community of Organisms Harmful to Plants or Plant Products and against their Spread within the Community. vol. 184.

Cao, Y., Raith, M.R., Griffith, J.F., 2015. Droplet digital PCR for simultaneous quantification of general and human-associated fecal indicators for water quality assessment. Water Res. 70, 337–349. https://doi.org/10.1016/j.watres.2014.12.008.

Cruaud, A., Gonzalez, A.-A., Godefroid, M., Nidelet, S., Streito, J.-C., Thuillier, J.-M., Rossi, J.-P., Santoni, S., Rasplus, J.-Y., 2018. Using insects to detect, monitor and predict the distribution of Xylella fastidiosa: a case study in Corsica. Sci. Rep. 8, 15628. https://doi.org/10.1038/s41598-018-33957-z.

Denancé, N., Legendre, B., Briand, M., Olivier, V., de Boisseson, C., Poliakoff, F., Jacques, M.-A., 2017. Several subspecies and sequence types are associated with the emergence of Xylella fastidiosa in natural settings in France. Plant Pathol. 66, 1054–1064. https://doi.org/10.1111/ppa.12695.

Doi, H., Takahara, T., Minamoto, T., Matsuhashi, S., Uchii, K., Yamanaka, H., 2015. Droplet digital polymerase chain reaction (PCR) outperforms real-time PCR in the detection of environmental DNA from an invasive fish species. Environ. Sci. Technol. 49, 5601–5608. https://doi.org/10.1021/acs.est.5b00253.

Dong, G., Meng, F., Zhang, Y., Cui, Z., Lidan, H., Chang, S., Zhao, P., 2018. Development and evaluation of a droplet digital PCR assay for the detection of fowl adenovirus serotypes 4 and 10 in attenuated vaccines. J. Virol. Methods. https://doi.org/10.1016/j.jviromet.2018.09.005.

Dreo, T., Pirc, M., Ramšak, Ž., Pavšič, J., Milavec, M., Žel, J., Gruden, K., 2014. Optimising droplet digital PCR analysis approaches for detection and quantification of bacteria: a case study of fire blight and potato brown rot. Anal. Bioanal. Chem. 406, 6513–6528. https://doi.org/10.1007/s00216-014-8084-1.

EFSA, 2018. Update of the Xylella spp. host plant database. EFSA J. 16. https://doi.org/10.2903/j.efsa.2018.5408.

EPPO, 2009. PM 7/97 (1): indirect immunofluorescence test for plant pathogenic bacteria. EPPO Bull 39. https://doi.org/10.1111/j.1365-2338.2009.02344.x.

EPPO, 2014. PM 7/98 (2) specific requirements for laboratories preparing accreditation for a plant pest diagnostic activity. EPPO Bull 44. https://doi.org/10.1111/epp.12118.

EPPO, 2018a. EPPO A2 List of Pests Recommended for Regulation as Quarantine Pests - Version 2018–09. WWW Document. https://www.eppo.int/ACTIVITIES/plant_quarantine/A2_list, Accessed date: 12 April 2018.

EPPO, 2018b. PM 7/24 (3) Xylella fastidiosa. EPPO Bull 48, 175–218. https://doi.org/10.1111/epp.12469.

FAOSTAT, 2017. Production quantities of Almonds, with shell by country. URL. http://www.fao.org/faostat/en/#data/QC/visualize, Accessed date: 5 June 2019.

Francis, M., Lin, H., Cabrera-La Rosa, J., Doddapaneni, H., Civerolo, E.L., 2006. Genome-based PCR primers for specific and sensitive detection and quantification of Xylella fastidiosa. Eur. J. Plant Pathol. https://doi.org/10.1007/s10658-006-9009-4.

Harper, S.J., Ward, L.I., Clover, G.R.G., 2010. Development of LAMP and real-time PCR methods for the rapid detection of Xylella fastidiosa for quarantine and field applications. Phytopathology 100, 1282–1288. https://doi.org/10.1094/PHYTO-06-10-0168.

Hayden, R.T., Gu, Z., Ingersoll, J., Abdul-Ali, D., Shi, L., Pounds, S., Caliendo, A.M., 2013. Comparison of droplet digital PCR to real-time PCR for quantitative detection of cytomegalovirus. J. Clin. Microbiol. 51, 540–546. https://doi.org/10.1128/JCM.02620-12.

Hindson, B.J., Ness, K.D., Masquelier, D.A., Belgrader, P., Heredia, N.J., Makarewicz, A.J., Bright, I.J., Lucero, M.Y., Hiddessen, A.L., Legler, T.C., Kitano, T.K., Hodel, M.R., Petersen, J.F., Wyatt, P.W., Steenblock, E.R., Shah, P.H., Bousse, L.J., Troup, C.B., Mellen, J.C., Wittmann, D.K., Erndt, N.G., Cauley, T.H., Koehler, R.T., So, A.P., Dube, S., Rose, K.A., Montesclaros, L., Wang, S., Stumbo, D.P., Hodges, S.P., Romine, S., Milanovich, F.P., White, H.E., Regan, J.F., Karlin-Neumann, G.A., Hindson, C.M., Saxonov, S., Colston, B.W., 2011. High-throughput droplet digital PCR system for absolute quantitation of DNA copy number. Anal. Chem. 83, 8604–8610. https://doi.org/10.1021/ac202028g.

Hoshino, T., Inagaki, F., 2012. Molecular quantification of environmental DNA using microfluidics and digital PCR. Syst. Appl. Microbiol. 35, 390–395. https://doi.org/10.1016/j.syapm.2012.06.006.

Huggett, J.F., Foy, C.A., Benes, V., Emslie, K., Garson, J.A., Haynes, R., Hellemans, J., Kubista, M., Mueller, R.D., Nolan, T., Pfaffl, M.W., Shipley, G.L., Vandesompele, J., Wittwer, C.T., Bustin, S.A., 2013. The digital MIQE guidelines: minimum information for publication of quantitative digital PCR experiments. Clin. Chem. 59, 892–902. https://doi.org/10.1373/clinchem.2013.206375.

Implementation Decision 2017/2352, 2017. DÉCISION D'EXÉCUTION (UE) 2017/2352 DE LA COMMISSION - du 14 décembre 2017 - modifiant la décision d'exécution (UE) 2015/789 relative à des mesures visant à éviter l'introduction et la propagation dans l'Union de Xylella fastidiosa (Wells et al.) - [notifiée sous le numéro C (2017) 8356]. J. Off. Union Eur 14.

Košir, A.B., Spilsberg, B., Holst-Jensen, A., Žel, J., Dobnik, D., 2017. Development and inter-laboratory assessment of droplet digital PCR assays for multiplex quantification of 15 genetically modified soybean lines. Sci. Rep. 7, 8601. https://doi.org/10.1038/s41598-017-09377-w.

Landa, B., 2017. Emergence of Xylella Fastidiosa in Spain: Current Situation. Presentation Made at the European Conference on Xylella 2017. WWW Document. https://www.efsa.europa.eu/en/events/event/171113, Accessed date: 17 January 2019.

Li, W., Teixeira, D.C., Hartung, J.S., Huang, Q., Duan, Y., Zhou, L., Chen, J., Lin, H., Lopes, S., Ayres, A.J., Levy, L., 2013. Development and systematic validation of qPCR assays for rapid and reliable differentiation of Xylella fastidiosa strains causing citrus variegated chlorosis. J. Microbiol. Methods 92, 79–89. https://doi.org/10.1016/j.mimet.2012.10.008.

Lievens, A., Jacchia, S., Kagkli, D., Savini, C., Querci, M., 2016. Measuring digital PCR quality: performance parameters and their optimization. PLoS One 11, e0153317. https://doi.org/10.1371/journal.pone.0153317.

Lu, Y., Zhang, H., Wen, C., Wu, P., Song, S., Yu, S., Luo, L., Xu, X., 2019. Application of droplet digital PCR in detection of seed-transmitted pathogen Acidovorax citrulli. J. Integr. Agric. 1688. https://doi.org/10.1016/S2095-3119(19)62673-0.

Maheshwari, Y., Selvaraj, V., Hajeri, S., Yokomi, R., 2017. Application of droplet digital PCR for quantitative detection of Spiroplasma citri in comparison with real time PCR. PLoS One 12, e0184751. https://doi.org/10.1371/journal.pone.0184751.

Martinetti, D., Soubeyrand, S., 2019. Identifying lookouts for epidemio-surveillance: application to the emergence of Xylella fastidiosa in France. Phytopathology 109, 265–276. https://doi.org/10.1094/PHYTO-07-18-0237-FI.

Minsavage, G., Thompson, C., Hopkins, D., Leite, R., Stall, R., 1994. Development of a polymerase chain reaction protocol for detection of Xylella fastidiosa in plant tissue. Phytopathology 84, 456. https://doi.org/10.1094/Phyto-84-456.

Modesti, V., Pucci, N., Lucchesi, S., Campus, L., Loreti, S., 2017. Experience of the Latium region (Central Italy) as a pest-free area for monitoring of Xylella fastidiosa: distinctive features of molecular diagnostic methods. Eur. J. Plant Pathol. 148, 557–566. https://doi.org/10.1007/s10658-016-1111-7.

Morisset, D., Štebih, D., Milavec, M., Gruden, K., Žel, J., 2013. Quantitative analysis of food and feed samples with droplet digital PCR. PLoS One 8, e62583. https://doi.org/10.1371/journal.pone.0062583.

Morley, A.A., 2014. Digital PCR: a brief history. Biomol. Detect. Quantif. 1, 1–2. https://doi.org/10.1016/j.bdq.2014.06.001.

Nixon, G., Alexander Garson, J., Grant, P., Nastouli, E., Foy, C., Huggett, J., 2014. Comparative study of sensitivity, linearity, and resistance to inhibition of digital and nondigital polymerase chain reaction and loop mediated isothermal amplification assays for quantification of human cytomegalovirus. Anal. Chem. 86. https://doi.org/10.1021/ac500208w.

Nunney, L., Schuenzel, E.L., Scally, M., Bromley, R.E., Stouthamer, R., 2014. Large-scale Intersubspecific recombination in the plant-pathogenic bacterium Xylella fastidiosa is associated with the host shift to mulberry. Appl. Environ. Microbiol. 80, 3025–3033. https://doi.org/10.1128/AEM.04112-13.

Ouyang, P., Arif, M., Fletcher, J., Melcher, U., Corona, F.M.O., 2013. Enhanced reliability and accuracy for field deployable bioforensic detection and discrimination of Xylella fastidiosa subsp. pauca, causal agent of citrus variegated chlorosis using razor ex technology and TaqMan quantitative PCR. PLoS One 8, e81647. https://doi.org/10.1371/journal.pone.0081647.

Rački, N., Dreo, T., Gutierrez-Aguirre, I., Blejec, A., Ravnikar, M., 2014. Reverse transcriptase droplet digital PCR shows high resilience to PCR inhibitors from plant, soil and water samples. Plant Methods 10. https://doi.org/10.1186/s13007-014-0042-6.

Ramírez, J.D., Herrera, G., Muskus, C., Mendez, C., Duque, M.C., Butcher, R., 2019. Development of a digital droplet polymerase chain reaction (ddPCR) assay to detect Leishmania DNA in samples from cutaneous Leishmaniasis patients. Int. J. Infect. Dis. 79, 1–3. https://doi.org/10.1016/j.ijid.2018.10.029.

Saponari, M., Boscia, D., Nigro, F., Martelli, G.P., 2013. Identification of DNA sequences related to Xylella fastidiosa in oleander, almond and olive trees exhibiting leaf scorch symptoms in Apulia (southern Italy). J. Plant Pathol. 95. https://doi.org/10.4454/JPP.V95I3.035.

Saponari, M., Giampetruzzi, A., Loconsole, G., Boscia, D., Saldarelli, P., 2019. Xylella fastidiosa in olive in Apulia: where we stand. Phytopathology 109, 175–186. https://doi.org/10.1094/PHYTO-08-18-0319-FI.

Schaad, N.W., Postnikova, E., Lacy, G., Fatmi, M., Chang, C.-J., 2004. Xylella fastidiosa subspecies: X. fastidiosa subsp piercei, subsp. nov., X. fastidiosa subsp. multiplex subsp. nov., and X. fastidiosa subsp. pauca subsp. nov. Syst. Appl. Microbiol. 27, 290–300. https://doi.org/10.1078/0723-2020-00263.

Schrader, C., Schielke, A., Ellerbroek, L., Johne, R., 2012. PCR inhibitors – occurrence, properties and removal. J. Appl. Microbiol. 113, 1014–1026. https://doi.org/10.1111/j.1365-2672.2012.05384.x.

Schuenzel, E.L., Scally, M., Stouthamer, R., Nunney, L., 2005. A multigene phylogenetic study of clonal diversity and divergence in north American strains of the plant pathogen Xylella fastidiosa. Appl. Environ. Microbiol. 71, 3832–3839. https://doi.org/10.1128/AEM.71.7.3832-3839.2005.

Voegel, T.M., Nelson, L.M., 2018. Quantification of agrobacterium vitis from grapevine nursery stock and vineyard soil using droplet digital PCR. Plant Dis. 102, 2136–2141. https://doi.org/10.1094/PDIS-02-18-0342-RE.

Vogelstein, B., Kinzler, K.W., 1999. Digital PCR. Proc. Natl. Acad. Sci. U. S. A. 96, 9236–9241.

Wang, M., Yang, J., Gai, Z., Huo, S., Zhu, J., Li, J., Wang, R., Xing, S., Shi, G., Shi, F., Zhang, L., 2018. Comparison between digital PCR and real-time PCR in detection of *Salmonella typhimurium* in milk. Int. J. Food Microbiol. 266, 251–256. https://doi.org/10.1016/j.ijfoodmicro.2017.12.011.

Wei, T., Lu, G., Clover, G., 2008. Novel approaches to mitigate primer interaction and eliminate inhibitors in multiplex PCR, demonstrated using an assay for detection of three strawberry viruses. J. Virol. Methods 151, 132–139. https://doi.org/10.1016/j.jviromet.2008.03.003.

Zhao, Y., Xia, Q., Yin, Y., Wang, Z., 2016. Comparison of droplet digital PCR and quantitative PCR assays for quantitative detection of Xanthomonas citri Subsp. citri. PLoS One 11, e0159004. https://doi.org/10.1371/journal.pone.0159004.